Raman and FTIR spectroscopy experimental and theoretical in magnetic nanoemulsion from *Carapa guianensis Aublet*

L.G.F. Silva[a,b,i], Q.S. Martins[c,*,ii], A. Ribas[c,iii], D.L.L. Oliveira[c], R.C.S Lima[c], and J.G. Santos[d,iv]

[a]*Programa em Nanociência e Nanobiotecnologia, Universidade de Brasília - UnB, Brasília, Brazil.*
[b]*Instituto Federal de Educação, Ciência e Tecnologia - IFRO, Porto Velho - RO, Brazil.*
[c]*Departamento de Física, Fundação Universidade Federal de Rondônia - UNIR, Ji-Paraná - RO, Brazil.*
[*]*e-mail: quesle.martins@unir.br*
[d]*Departamento de Física, Fundação Universidade Federal de Rondônia - UNIR, Porto Velho - RO, Brazil.*

Received 10 February 2023; accepted 21 March 2023

This work brings Raman and Fourier transform infrared (FTIR) spectroscopy as a proposal for a vibrational characterization of *Carapa guianensis Aublet* essential oil in natura and polymerized and of magnetic nanoemulsion. Calculation of computational chemistry based on the method density functional theory with B3LYP functional and 6-311+G** base set parameters was used to obtain theoretical frequencies and vibrational signatures of the oleic acid molecule. Results of Raman and Fourier transform infrared spectroscopy confirm bands of *Carapa guianensis Aublet* essential oil present in polymerized oil and magnetic nanoemulsion studied. The density functional theory method shows that the bands 1099 cm^{-1}, 1714 cm^{-1} and 1812 cm^{-1} explain the presence of vibrational modes of oleic acid in the samples. The density functional theory brought good conformation to the chosen molecule.

Keywords: Nanoemulsion; amazonian oil; vibrational spectroscopy; density functional theory method.

DOI: https://doi.org/10.31349/RevMexFis.69.051003

1. Introduction

Andiroba is the popular name of *Carapa guianensis Aublet*. From Amazonian origin, vegetable oil rich in polyunsaturated fatty acids (PUFA) is extracted from it [1–5]. Such compounds in natural oils are often labeled with phytotherapy [6, 7], associated with anti-inflammatory, antibacterial and antifungal properties [8–10]. With such characteristics, andiroba oil has enormous potential for application. In view of this, the study for the development of oil-based nano emulsions of vegetable origin is highly encouraged [11, 12]. Nano emulsions are dispersions of two or more immiscible fluids where at least one of their components is on a nano-scale. Among their characteristics, they can present good versatility and high interaction with external magnetic fields, such as those constituted by a polymeric matrix doped with nanoparticles, based on ferrite magnets and diluted in aqueous solution. This type of compound generates interest in permeation and vectoring studies in the delivery of drugs, in addition to other biological applications [13–18]. In this study, Raman spectroscopy (Raman) and Fourier transform infrared spectroscopy (FTIR) in essential oil of *Carapa guianensis Aublet* in natura (CGEO) and polymerized (CGPO) and nano emulsion (CGNE) developed from Polymerized material was applied. FTIR and Raman are important tools in determining functional groups linked to molecules and atoms, besides having as an advantage, fast data acquisition, with high precision and complementarity of the active modes in each of them [19–23]. A computational approach was added by incorporating the oleic acid molecule. The Density Functional Theory (DFT) was the method chosen. Thus, molecular optimization, the calculated frequencies and spectra of the oleic acid molecule (OA) were obtained, which were compared with experimental results. OA was chosen because it was a major component in a higher proportion for CGEO [24]. The B3LYP functional and 6-311+G** basis were used, since they best fit the types of atoms involved [25–27]. In addition, additional information has been obtained in VEDA software. The calculation generated theoretical spectra and vibrational signature data that were compared with experimental results. The experimental results indicate that all samples present bands related to the OA molecule, especially for bands of C=C and C=O. These results express that the components of CGEO are still present in the studied samples. The DFT method was successful in predicting important bands of the molecule studied. The importance of the study is directed to the field of applied sciences, since there are no reports of the application of this methodology to the study of CGEO based nano emulsions. The study is a pioneer in combining experimental techniques and computational modeling in the development of a CGEO-based nano emulsion.

2. Materials and methods

2.1. Synthesis of nanoemulsion

The CGEO was obtained from a producers cooperative (Associação de Produtores Agroextrativistas da Colônia do Sardinha, Lábrea-AM, Brazil). The essential oil-based polymer was synthesized using the polycondensation technique, where the triglyceride chain was broken using 1N Koh and free fatty acids polymerized using the ligand monomer

$C_2H_6O_4$ [28–31]. The nanoparticles were synthesized by a chemical precipitation technique using 1:2 $FeCl_3$-$6H_2O$ and $FeCl_2$-$4H_2O$ [32, 33]. Using an ultrasonic homogenization, an oil-in-water nanoemulsion was prepared, where nanoparticles are homogenized with the essential oil-based polymer, adding, in proportion 1:4, water and 0.4 g Tween 80 in an Ultrasonic Sonicator under 60 W and 20 kHz for 10 min.

2.2. Experimental

The Raman spectrum was acquired at Raman Labram HR 800 spectrometer, with 633.5 nm laser, in the range from 80 to 3400 cm^{-1} at the Light spreading Laboratory of the Federal University of Mato Grosso - UFMT. The FTIR acquired spectra were acquired using a SHIMADZU FTIR-IR-Prestige-21 spectrometer, in total attenuated reflectance (ATR) mode with the samples in liquid state. For analysis, one drop of each sample (without dilution) is deposited in a diamond crystal and the spectra were obtained in the region between 4.000 to 400 cm^{-1}, with a resolution of 4 cm^{-1} and 60 scans. Measurements were performed at the Laboratory of Characterization and Microscopy of Materials of Federal University of Alagoas UFAL. The experimental spectra were treated with Savitzky-Golay smoothing function in Origin software [34, 35].

2.3. Computational methods

Computational calculations were performed using the Gaussian 09 pack age, optimizing the structure and predicting the harmonic vibrational Raman and IR frequencies [36]. Functional B3LYP combined with a base set 6-6-311+G** or 311+G(d,p) was used. B3LYP is a three parameter function (B3) used for the Lee-Yang Parr (LYP) functional correlation exchange. The LYP correlation is a more cost-effective approach to calculating the molecular structure, vibrational frequencies, and energy of optimized structures [37–39]. The polarization used allows good optimization results in organic molecular groups. The 3 description of normal oleic acid modes was performed in terms of analysis of potential energy distribution (PED) using the VEDA software. The description of normal oleic acid modes was performed in terms of analysis of potential energy distribution (PED) using the VEDA 4 software [40]. The theoretical vibrational spectra were reduced with a scale factor of 0.967 to compensate for the resulting error of the vibrational disharmony and the incomplete electronic correlation of the treatment.

3. Results and discussion

3.1. Experimental

Figure 1 and 2 show FTIR and Raman of CGNE, CGPO and CGEO spectra (Also the calculated spectra of OA in line blue). Figure 1 shows the region between 4000 and 500 cm^{-1}. The CGEO spectrum is seen in red, CGPO in blue and CGNE in black. FTIR bands present markings for OH, CH, COC, C=O and CH_3 groups. FTIR of CGEO shows bands in 2935, 2853, 1743 cm^{-1} and in 1235 e 725 cm^{-1}. The spectrum of CGPO Fig. 1 shows bands in 3299, 2935 and 2853 cm^{-1} (associated with CH_2 and CH_3), 1411 cm^{-1} (linked to vibrations CH_3), 1161 cm^{-1} and 1093 cm^{-1} (OCC group). For CGNE the main bands are in 3299, 1550 and 680 cm^{-1} regions. The results show that CGPO and CGNE contain bands at 3299 cm^{-1}, a broad and intense band common to OH stretching. We can also see bonded bands CH_2 and CH_3 (methyl group) in 2935 and 2853 cm^{-1} for CGPO and CGEO.

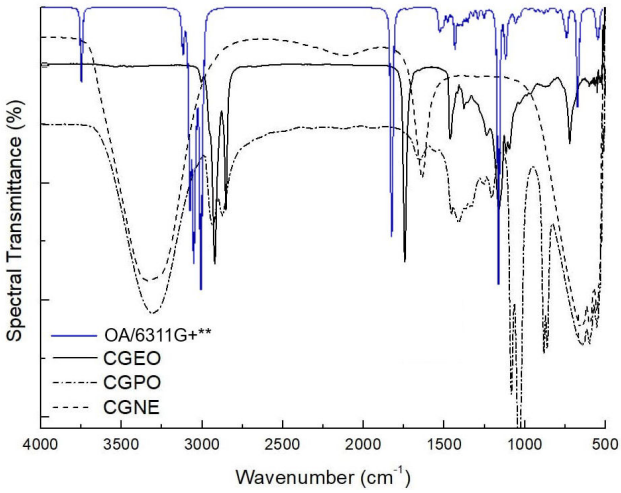

FIGURE 1. Fourier transformed infrared spectra of the *Carapa guianensis Aublet* oil, Carapa Guianensis polymer and magnetic nanoemulsion in continuous line, dash-dot and dash respectively. Calculate FTIR spectrum of the oleic acid molecule in blue. The B3LYP/6-311G+** or 6-311G+(d,p) was used.

The region between 4000-2800 cm^{-1} shows that CGEO does not contain OH band (3299 cm^{-1}) and CGNE does not show CH_2 and CH_3 bands. In the region between 2000-1000 cm^{-1} we have an intense and thin band at 1743 cm^{-1} for CGEO, indicating the presence of C=O stretch. Just below, in the region of 1628 cm^{-1}, CGPO and CGNE show bands of the C-O grouping. Below 1250 cm^{-1}, the CGPO shows a band combined with marking at 1090 cm^{-1} and 1030 cm^{-1} associated with C-O-C groups vibrations The bonding of CO esters are indicators on 1235 cm^{-1} of CGEO [41–43]. The region between 750-500 cm^{-1}, shows a CH band at 725 cm^{-1} for CGEO. Considering carboxylic acid a long chain grouping, the band is associated with 725 cm^{-1}, present in this type of structure [42, 44, 50]. Whereas for CGPO and CGNE, we see a broad band between 900-500 cm^{-1} that may be associated with oxygen interactions with other compounds in dispersion, as is the case with ferrite magnets. As the CGPO is the fruit of the polymerization process, we can see that the FTIR spectrum shows that few bands were preserved in relation to essential oil, except for the CH bands in 2935, e 2853 cm^{-1}. The new bands found are related to the new synthesized polymer. In this case, the ligand monomer used in the CGEO polymerization process

was Ethylene Glycol (EG), whose synthesized compound is a derivative of Polyethylene Glycol (PEG) [45]. The main bands are OH (3299 cm^{-1}), COO (1628 cm^{-1}) and COC (1090 and 1030 cm^{-1}). When analyzing the data obtained from FTIR of the synthesized polymer, it was observed that the predominant bands are similar to the PEG visited. The FTIR spectrum of CGNE follows this trend. In CGNE there are bands associated with OH and CO bonding, as in CGPO, in addition to vibrations bands in the region ranging from 750 to 500 cm^{-1} [43]. In this case, the absence of CH bands around 2850 cm^{-1} and the appearance of a band centered at 1550 cm^{-1} and a band between 750-500 cm^{-1}, which may be associated with the interactions of FeO oxygen with other compounds in dispersion. This may explain the band enlargement, as reported for magnets ferrites [46]. Figure 2 shows the Raman of the CGEO, CGPO and CGNE samples. It is observed that the results bring in the region of digital printing, a set of 5 to 6 medium intensity bands for CGEO and CGPO, very common vegetable oils spectra [47]. These bands are at 1080 cm^{-1}, 1302 cm^{-1} and 1438 cm^{-1}, referring to groups of -CH_2. In 1657 cm^{-1} a typical band for C=C and C-H bonds, common in unsaturated fatty acids, is associated with symmetrical stretching modes [48, 49]. In 1749 cm^{-1} for CGEO and CGPO samples we have a band associated with carbonyl group stretching (C=O). The band at 1749 cm^{-1} can be easily noticed in the spectra in the FTIR measurements in Fig. 1, because it is an intense and narrow band. Bands common to CH groups appear above 2500 cm^{-1}. Thus, bands in 2724 cm^{-1}, 2848 cm^{-1}, 2893 cm^{-1} and 3007 cm^{-1} are associated with -CH and -CH_3 bonding [50, 51]. In the Raman spectrum of CGNE there is a total or partial suppression of the bands for a wide fluorescence curve, as seen mainly in the region between 300-1800 cm^{-1}, which indicates the enveloping of the bands present. In the vicinity of 3000 cm^{-1}, a set of bands are noted that refer to the existing CH groups.

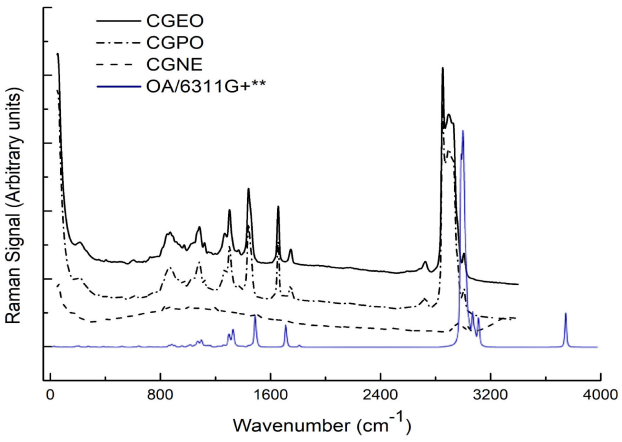

FIGURE 2. Raman spectra of the *Carapa guianensis Aublet* oil (CGEO), Carapa Guianensis polymer (CGPO) and magnetic nanoemulsion (CGNE). Calculate Raman spectrum of the oleic acid molecule In blue. The B3LYP/6-311G+** or 6-311G+(d,p) was used.

Still in CGNE, above 3200 cm^{-1}, a mild elevation, may indicate the presence of OH modes. In studies already mentioned [52–54], there are no references of a broadband in this region for vegetable oils, even if they contain fatty acids, which have the hydroxyl radical (Fig. 3), something appears for the calculated spectra (see Fig. 1). Below 500 cm^{-1}, all the spectra show a band with common characteristics. For CGEO and CGPO we have the band at 238 cm^{-1} and CGNE is at 210 cm^{-1} region. All the samples show a band at 372 cm^{-1}, associated with CC deformations.

3.2. Calculation

Figure 3 is the oleic acid structure, belonging to the group of C1 points of symmetry.

It has 156 fundamental vibrations expressed by 53 stretching (υ), 52 bending (δ) and 51 torsions (τ), which have been assigned with the VEDA software. The vibrational assignment of normal molecule modes was performed based on PED analysis. Only PED values greater than 10% are provided [40]. Table I shows the acquired vibrational data, including the calculated fundamental harmonic frequencies and their corresponding scale values are compared with the experimental Raman and FTIR wavenumber. The calculated spectra of OA with functional B3LYP and 6-311G+** base set are also shown in Figs. 1 and 2 (blue line) for facilitate comparison. In Fig. 1 (blue line) the intense band of C=O bonding appears at 1832 cm^{-1} for FTIR spectrum. This band appears less intense in Raman (Fig. 2 - blue line). This situation shows how symmetric or non-symmetric groups can be distinct in both techniques. The situation is similar when checking the band at 1714 cm^{-1} in calculated Raman. It appears narrow and intense in calculated Raman, but in calculated FTIR this band is practically omitted. In Fig. 1, around 3000 cm^{-1} the bands related to CH groups have similar, intense and fractionated profiles. The highlight is the band centered at 3083 cm^{-1} which is intense in both spectra. Still in Fig. 1, in 3759 cm^{-1} we have bands that indicate symmetrical stretching modes of OH. In the experimental spectra this band is not present for CGEO and CGPO. Whereas for CGNE, the presence of broadband may be evidence of the sample's OH groups [23, 42, 50]. The bands in 636 and 647 cm^{-1} are linked to carboxyl grouping with formation mode and torsion respectively, as seen in Table I. These groups may indicate that in CGEO and CGPO, they may be responsible for the low intensity band in the region of 636 cm^{-1}.

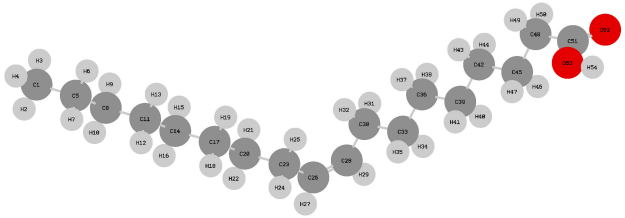

FIGURE 3. Oleic acid structure ($C_{18}H_{34}O_2$) optimized in Gaussian 09. In red is oxygen, light gray, hydrogen and gray, carbon.

TABLE I. FTIR and Raman experimental and theoretical modes of the B3LYP/6-311G+** parameters calculated oleic acid molecule and assignments. Percentage (%) of vibrational contribution given by VEDA software.

Experimental		Theoretical		Assignments (PED%)
ω_{IR}	ω_{Raman}	ω_{calc}	ω_{scal}	
3299	-	3759	3635	υ_sOH(1 54) (100)
-	-	3123	3020	υ_sCH$_{cis}$(17 48) (58)
-	-	3098	2996	υ_{as}CH$_{cis}$(16 47) (56)
-	3007	3083	2981	υ_{as}CH$_3$(19 52) (74)
-	-	3078	2976	υ_{as}CH$_3$(19 51) (43)
-	-	3077	2975	υ_{as}CH$_2$(12 40) (63)
-	-	3054	2953	υ_{as}CH$_2$(18 49 50) (27)
2935	-	3037	2937	υ_sCH$_2$(14 43) (37)
-	-	3017	2917	υ_sCH$_3$(19 51) (37)
-	-	3009	2910	υ_sCH$_2$(8 32 31) (27)
2853	2893	2993	2894	υ_sCH(3 22) (38)
-	2724	-	-	*Undefined*
1743	1749	1812	1752	υ_sC=O(2 20) (85)
1628	1657	1714	1657	υ_sC=C(17 16) (72)
1460	-	1514	1464	δ_{sci}CH$_2$(26 5 25) (19)
-	1438	1488	1439	δ_{sci}CH$_2$(46 15 45) (23)
1411	-	1414	1367	δ_{sci}CH$_2$(52 19 51) (31)
-	1302	1352	1307	δ_wCH(40 12 16 17) (21)
-	-	1325	1281	δ_tCH$_2$(27 6 9) (14)
1235	-	1237	1196	δ_rCH(41 13 17) (13)
-	-	1143	1105	υ_sOC(1 20) (31)
1093	1080	1099	1063	υ_sCC(18 14) (11)
1030	-	1071	1035	υ_sCC(11 5) (27)
937	-	957	925	υ_sCC(13 17) (27)
725	-	647	626	τOHCC(54 1 20 18) (55)
-	636	636	615	δ_{sci}OC=O(2 20 1) (60)
-	372	380	367	δCCC(4 8 12) (24)
-	238	200	193	δCCC(8 12 16) (23)
-	210	182	176	δCCC(9 13 17) (10)

Symmetrical (υ_s), asymmetrical (υ_{as}), scissor (δ_{sci}), twist (δ_t), wagg (δ_w), rock (δ_r) and torsion (τ).

Table I presents a combination of experimental and calculated frequencies. The frequencies are accompanied by the vibrational signatures and percentage of contribution given by PED. Frequencies are labeled with ω. PED contributions with a value of 10% or more were indicated. In the PED analysis performed automatically by VEDA for the oleic acid, the EPM parameter reached 27.43. The EPM is the optimization parameter value, which is the arithmetic mean of the maximum elements of each column of the PED matrix [55]. The calculated frequencies were chosen to be consistent with the experimental data. In addition to experimental and calculated frequencies, Table I also brings staggered frequencies. The theoretical vibrational spectra were reduced with a scale factor of 0.967 to compensate for the resulting error of the vibrational disharmony and the incomplete electronic correlation of the treatment, as indicated in CCCBDB [56,57]. The DFT method was successful in predicting important bands of oleic acid, allowing the assignment of vibrational modes to *Carapa guianensis Aubl*.

4. Conclusion

Raman and FTIR spectra showed bands of CGEO and CGPO and CGNE specific to each sample. CGEO bands were preserved in CGPO and CGNE. FTIR spectra are clear for all the samples indicating the stage each of them has been subjected

to. In FTIR of CGEO, the esterification process determined the predominance of PEG bands combined with CGEO. In Raman, the CGNE data are not clear. However, bands between 2300 and 2500 cm^{-1} regions that indicate the presence of CH_2 and CH_3 bands are preserved. The results indicate that all samples present bands related to the OA molecule, especially for bands of C=C and C=O. These results express that the components of CGEO are still present in the studied samples. The study may subsidize future research on nano emulsions, since natural polymer nano emulsions are of great scientific and community interest.

Author statement

L.G.F Silva, Q.S. Martins: Conceptualization, Methodology, Project administration, Writing - Original Draft. L.G.F Silva, Q.S. Martins: Data curation, Visualization, Investigation, Writing - Original draft preparation. R.C.S Lima, D.L.L. Oliveira, A. Ribas: Visualization. L.G.F Silva, Q.S. Martins: Software, Validation, Data curation. L.G.F Silva, J.G. Judes: Supervision, Project administration, Methodology, Writing Reviewing and Editing. Declaration of interests The authors declare no conflict of interest relationship in this paper.

Acknowledgments

The authors acknowledges the was financially and academic support offered by PhD Program in Nanoscience and Nanobiotechnology, the PIBIC-CNPQ and FAPERO 009/2022. The Optics and Nanoscopy Group (GON) - UFAL, Laboratório de Espalhamento de Luz - UFMT. The reserach group Física Experimental e Aplicada - UNIR and Estrutura da Matéria e Física Computacional DAF/JP - UNIR.

---

i. https://orcid.org/0000-0003-3958-8430.

ii. https://orcid.org/0000-0002-1315-2164.

iii. https://orcid.org/0000-0002-9115-4755.

iv. https://orcid.org/0000-0002-2339-1417.

1. C.A. Martin *et al*., Omega-3 and omega-6 polyunsaturated fatty acids: importance and occurrence in foods, *Rev. Nutr.* **19** (2006) 761, https://doi.org/10.1590/S1415-52732006000600011.

2. Q. Shu-Hua, W. Da-Gang, M. Yun-Bao and L. Xiao-Dong, A Novel Flavane from Carapa guianensis *J Integr Plant Biol.*, **9** (2003) 1129, https://www.jipb.net/EN/Y2003/V45/I9/1129.

3. C.A. Klimas, K.A. Kainer and L.H.O. Wadt, Population structure of Carapa guianensis in two forest types in the southwestern Brazilian Amazon, *For. Ecol. Manage.*, **3** (2007) 256, https://doi.org/10.1016/j.foreco.2007.05.025.

4. M.R.A. Ferreira *et al*., Development and Evaluation of Emulsions from Carapa guianensis (Andiroba) *Oil. AAPS PharmSciTech*, **11** (2010) 1383, https://doi.org/10.1208/s12249-010-9491-z.

5. K.K. Barros Dias *et al*., Biological activities from andiroba (Carapa guianensis Aublet.) and its biotechnological applications: A systematic review, *Arab. J. Chem.*, **4** (2023) 104629, https://doi.org/10.1016/j.arabjc.2023.104629.

6. S. Gordon I *et al*., Dietary omega-3 fatty acid supplementation increases the rate of muscle protein synthesis in older adults: a randomized controlled trial, *Am. J. Clin. Nutr.* **9** (2011) 402, https://doi.org/10.3945/ajcn.110.005611.

7. S. Gavanji, B. Larki, and A. Hosein, A review of Application of Ostrich oil in Pharmacy and Diseases treatment, *J. Nov. Appl. Sci.*, **18** (2013) 650, https://jnasci.org/2013-2-11/.

8. H. Ali, H. Nawaz, M. Saleem, F. Nurjis, and M. Ahmed, Qualitative analysis of desi ghee, edible oils, and spreads using Raman spectroscopy, *J. Raman Spectrosc.*, **47** (2016) 706, https://doi.org/10.1002/jrs.4891,

9. W. Dong, Y. Zhang, B. Zhang, and X. Wang, Rapid prediction of fatty acid composition of vegetable oil by Raman spectroscopy coupled with least squares support vector machines, *J. Raman Spectrosc*, **44** (2013) 1739, https://doi.org/10.1002/jrs.4386,

10. V. Baeten, P. Hourant, M. T. Morales, and R. Aparicio, Detection of Virgin Olive Oil Adulteration by Fourier Transform Raman Spectroscopy, *Agric. Food Chem.* **44** (1996) 2225, https://doi.org/10.1021/jf9600115.

11. G. Ledet, S. Pamujula, V. Walker, S. Simon, R. Graves, and T.K. Mandal, Development and in vitro evaluation of a nanoemulsion for transcutaneous delivery, *Drug Dev. Ind. Pharm.*, **40** (2014) 370, https://doi.org/10.3109/03639045.2012.763137.

12. R.K. Harwansh, K.C. Patra, S.K. Pareta, J. Singh, and M.A. Rahman, Nanoemulsions as vehicles for transdermal delivery of glycyrrhizin, *Braz. J. Pharm. Sci.*, **47** (2011) 769, https://doi.org/10.1590/S1984-82502011000400014.

13. A.M. Cardoso *et al*., Chitosan hydrogels containing nanoencapsulated phenytoin for cutaneous use: Skin permeation/penetration and efficacy in wound healing. *Mater. Sci. Eng.*, **96** (2019) 205, https://doi.org/10.1016/j.msec.2018.11.013.

14. L.A. Huber *et al*., Topical skin cancer therapy using doxorubicin-loaded cationic lipid nanoparticles and iontophoresis, *J. Biomed. Nanotechnol*, **11** (2015) 1975, https://doi.org/10.1166/jbn.2015.2139,

15. F. Bruxel *et al*., Nanoemulsions as parenteral drug delivery systems, *Quim. Nova*, **35** (2012) 1827, https://doi.org/10.1590/S0100-40422012000900023.

16. T.W. Prow *et al*., Nanoparticles and microparticles for skin drug delivery, *Adv. Drug Deliv. Rev.*, **63** (2011) 470, https://doi.org/10.1016/j.addr.2011.01.012.

17. S.R. Mudshinge, A.B. Deore, S. Patil, and C.M. Bhalgat, Nanoparticles: Emerging carriers for drug delivery, *Saudi Pharm. J.*, **19** (2011) 129, https://doi.org/10.1016/j.jsps.2011.04.001.

18. M. Arruebo, R. Fernández-Pacheco, M. Ibarra, and J. Santamaría, Magnetic nanoparticles Controlled release of drugs from nanostructured functional materials, *Rev. - Lit. Arts Am.*, **2** (2007) 22, http://linkinghub.elsevier.com/retrieve/pii/S1748013207700841.

19. T. De Beer, A. Burggraeve, M. Fonteyne, L. Saerensa, J.P. Remon, and C. Vervaet, Near infrared and Raman spectroscopy for the in-process monitoring of pharmaceutical production processes, *Int. J. Pharm.* **30** (2011) 32, doi: https://doi.org/10.1016/j.ijpharm.2010.12.012.

20. C.B. Silva, J.G. da Silva Filho, G.S. Pinheiro, A.M.R. Teixeira, and P.T.C. Freire, Vibrational and structural properties of L-Alanyl-L-Phenylalanine dipeptide by Raman spectroscopy, infrared and DFT calculations, *Vib. Spectrosc.* **98** (2018) 128, https://doi.org/10.1016/j.vibspec.2018.08.001.

21. A. Abkari, I. Chaabane, and K. Guidara, DFT (B3LYP/LanL2DZ and B3LYP/6311G+(d,p)) comparative vibrational spectroscopic analysis of organic-inorganic compound bis(4-acetylanilinium) tetrachlorocuprate(II), *Physica E*, **81** (2016) 136, http://dx.doi.org/10.1016/j.physe.2016.03.010.

22. V. Baeten, Raman spectroscopy in lipid analysis, *Lipid Technol.*, **22** (2010) 36, https://doi.org/10.1002/lite.200900082.

23. Q. S. Martins, L. M. S. Santos, and J. L. B. Faria, Raman spectra and ab-initio calculations in Bertholletia excelsa oil, *Vib. Spectrosc.* **106** (2020) 102986, https://doi.org/10.1016/j.vibspec.2019.102986.

24. K.M. Melo, L.F. Oliveira, R.M. Rocha, and M.A. Pantoja, Andiroba oil and nanoemulsion (*Carapa Guianensis Aubl.*) reduce lesion severity caused by the antineoplastic agent doxorubicin in mice, *Biomed. Pharmacother.*, **138** (2021) 111505, https://doi.org/10.1016/j.biopha.2021.111505.

25. H. Lam, P.K. Roy, and S. Chattopadhyay, Thermal degradation in edible oils by surface enhanced Raman spectroscopy calibrated with iodine values, *Vib. Spectrosc.*, **106** (2020) 103018, https://doi.org/10.1016/j.vibspec.2019.103018.

26. P. Jayaraj, and R. Desikan, Synthesis, crystal structure, and DFT calculations of 2H-1,3-benzodioxol-5-yl 3-(4-hydroxy-3-methoxyphenyl) prop-2-enoate, *Chem. Data Collect.* **29** (2020) 100518, https://doi.org/10.1016/j.cdc.2020.100518.

27. V.V. Kuzmin, V.S. Novikov, L.Yu. Ustynyuk, K.A. Prokhorov, E.A. Sagitova, and G.Yu. Nikolaeva, Raman spectra of polyethylene glycols: Comparative experimental and DFT study, *J. Mol. Struct.*, **1217** (2020) 128331, https://doi.org/10.1016/j.molstruc.2020.128331.

28. S. Miao, P. Wang, Z. Su, and S. Zhang, Vegetable-oil-based polymers as future polymeric biomaterials. *Acta Biomater.*, **10** (2014) 1692, https://doi.org/10.1016/j.actbio.2013.08.040.

29. F.S Güner, Y. Yagcı, and A.T. Erciyes, Polymers from triglyceride oils, *Prog. Polym. Sci.*, **31** (2006) 633, https://doi.org/10.1016/j.progpolymsci.2006.07.001.

30. V. Sharma, and P.P. Kundu, Condensation polymers from natural oils, *Prog. Polym. Sci.*, **33** (2008) 1199, https://doi.org/10.1016/j.progpolymsci.2008.07.004.

31. L.G. Silva, T.A. Beleza, J.G. Santos, and L.B. Silveira, A Hybrid Nanocomposite from γ-Fe2O3 Nanoparticles Functionalized in the Amazon Oil Polymers matrix, *Int. J. Innov. Rduc. Res.*, **8** (2020) 418, https://doi.org/10.31686/ijier.vol8.iss6.2435.

32. A.B. Chin, and I. Yaacob, Synthesis and characterization of magnetic iron oxide nanoparticles via w/o microemulsion and Massart's procedure, *J. Mater. Process. Technol.*, **191** (2007) 235, https://doi.org/10.1016/j.jmatprotec.2007.03.011.

33. S. Laurent *et al*., Magnetic iron oxide nanoparticles: Synthesis, stabilization, vectorization, physicochemical characterizations and biological applications, *Chem. Rev.*, **108** (2008) 2064, https://doi.org/10.1021/cr068445e.

34. N. Abu-Khalaf and M. Hmidat, Visible/Near Infrared (VIS/NIR) spectroscopy as an optical sensor for evaluating olive oil quality, *Comput. Electron. Agric.*, **173** (2020) 105445, https://doi.org/10.1016/j.compag.2020.105445.

35. V.K. Redasani *et al*., A review on derivative uv-spectrophotometry analysis of drugs in pharmaceutical formulations and biological samples review, *J. Chil. Chem.*, **63** (2018) 4126, https://doi.org/10.4067/s0717-97072018000304126.

36. M.J. Frisch *et al*., *Gaussian* **09** (2009).

37. A. D. Becke, Density-functional thermochemistry. III. The role of exact exchange, *J. Chem. Phys.* **98** (1993) 5648, https://doi.org/10.1063/1.464913.

38. C. Lee, W. Yang, and R. G. Parr, Development of the Colle-Salvetti correlation-energy formula into a functional of the electron density, *Phys. Rev. B*, **98** (1988) 785, https://doi.org/10.1103/PhysRevB.37.785.

39. X. Wu, S. Gao, J. S. Wang, H. Wang, Y. W. Huanga, and Y. Zhaod, The surface-enhanced Raman spectra of aflatoxins: spectral analysis, density functional theory calculation, detection and differentiation, *Anlst.*, **137** (2012) 4226, https://doi.org/10.1039/C2AN35378D.

40. M.H. Jamróz, Vibrational Energy Distribution Analysis (VEDA): Scopes and limitations, *Spectrochim. Acta A Mol. Biomol. Spectrosc.*, **114** (2013) 220, https://doi.org/10.1016/j.saa.2013.05.096.

41. G.A. Senhorini, S.F. Zawadzki, P.V. Farago, S.M.W. Zanin, and F.A. Marques, Microparticles of poly(hydroxybutyrate-co-hydroxyvalerate) loaded with andiroba oil: Preparation and characterization, *Mater. Sci. Eng. C*, **5** (2012) 1121, https://doi.org/10.1016/j.msec.2012.02.027.

42. Q.S. Martins, C.A. Aguirre, and J. Farias, Approach by Raman and infrared spectroscopy in three vegetable oils from the Brazilian Amazon, *Rev. Mex. FÃs.*, **4** (2019) 328, https://doi.org/10.31349/RevMexFis.65.328.
43. D.F. Silva *et al*., PCL/Andiroba Oil (Carapa guianensis Aubl.) Hybrid Film for Wound Healing Applications, *Polymer.* **10** (2021) 1591, https://doi.org/10.3390/polym13101591.
44. F.B. de Santana, S.J. Mazivila, L.C. Gontijo, W.B. Neto, and R.J. Poppi, Rapid Discrimination Between Authentic and Adulterated Andiroba Oil Using FTIR-HATR Spectroscopy and Random Forest, *Food Anal. Methods* **11** (2018) 1927, https://doi.org/10.1007/s12161-017-1142-5.
45. NIST Standard Reference Database SRD Number 69. Last update to data: (2022) DOI: https://doi.org/10.18434/T4D303.
46. L.G.F. Silva, H. P. Pacheco, Q. S. Martins, J. G. Santos, and L. B. Silveira, Development of magneto-polymer nanoemulsions based on the amazon oil of carapa guianensis aubl, *Int. J. Dev. Res.* **12** (2022) 2573, https://doi.org/10.37118/ijdr.25736.11.2022.
47. F. Huang *et al*., Identification of waste cooking oil and vegetable oil via Raman spectroscopy, *J. Raman Spectrosc.* **47** (2016) 860, https://doi.org/10.1002/jrs.4895.
48. W. Rumińska, M. Szymańska-Chargot, D. Wiacek, A. Sobota, K.H. Markiewicz, and A. Nawrocka, FT-Raman and FT-IR studies of the gluten structure as a result of model dough supplementation with chosen oil pomaces, *J. Cereal Sci.* **93** (2020) 102961, https://doi.org/10.1016/j.jcs.2020.102961.
49. R. Hu, T. He, Z. Zhang, Y. Yang, and M. Liu, Safety analysis of edible oil products via Raman spectroscopy, Talanta, **191** (2019) 324, https://doi.org/10.1016/j.talanta.2018.08.074.
50. Q.S. Martins, P.V. Almeida, Q.S. Ferreira, A. Oliveira, C. Aguirre, and J.L.B. Faria, Investigation of ostrich oil via Raman and infrared spectroscopy and predictions using the DFT method, *Vib. Spectrosc.* **104** (2019) 102945, https://doi.org/10.1016/j.vibspec.2019.102945.
51. S. Saravanan, and V. Balachandran, Quantum mechanical study and spectroscopic (FT-IR, FT-Raman, UV-Visible) study, potential energy surface scan, Fukui function analysis and HOMO-LUMO analysis of 3-tert-butyl-4-methoxyphenol by DFT methods, *Spectrochim. Acta A Mol. Biomol. Spectrosc.*, **130** (2014) 604, https://doi.org/10.1016/j.saa.2014.04.058
52. T.K. Lima, M. Musso, and D.B. Menezes, Using Raman spectroscopy and an exponential equation approach to detect adulteration of olive oil with rapeseed and corn oil, *Food Chem.*, **333** (2020) 127454, https://doi.org/10.1016/j.foodchem.2020.127454.
53. P.V. Jentzsch and V. Ciobotă, Raman spectroscopy as an analytical tool for analysis of vegetable and essential oils, *Flavour Fragr. J.*, **29** (2014) 287, https://doi.org/10.1002/ffj.3203.
54. A.M. Marina, Y.B. Che Man, S.A.H. Nazimah, and I. Amin, Chemical Properties of Virgin Coconut Oil, *J. Am. Oil Chem. Soc.* **86** (2009) 301, https://doi.org/10.1007/s11746-009-1351-1.
55. M.H. Jamróz, S. Ostrowski, and J.Cz. Dobrowolski, Facilitation of the PED analysis of large molecules by using global coordinates, *Spectrochim. Acta A Mol. Biomol. Spectrosc.* **149** (2015) 463, http://dx.doi.org/10.1016/j.saa.2015.04.038.
56. R. D. Johnson III (Ed.), Computational Chemistry Comparison and Benchmark Database, NIST Standard Reference Database, Release 22, NIST, 2022. https://doi.org/10.18434/T47C7Z
57. J.A. Antunes et al., Study on optical, electrochemical and thermal properties of the Meldrum acid 5-aminomethylene derivative, *Vib. Spectrosc.* **112** (2021) 103188, https://doi.org/10.1016/j.vibspec.2020.103188.